Crooks Fluctuation Theorem for a Process on a Two-Dimensional Fluid Field

Julia Gundermann* and Holger Kantz
Max-Planck-Institut für Physik Komplexer Systeme, Nöthnitzer Strasse 38, 01187 Dresden, Germany

Jochen Bröcker
School of Mathematical and Physical Sciences, University of Reading,
Whiteknights, P.O. Box 220, Reading RG6 6AX, United Kingdom
(Received 14 January 2013; revised manuscript received 18 April 2013; published 7 June 2013)

We investigate the behavior of a two-dimensional inviscid and incompressible flow when pushed out of dynamical equilibrium. We use the two-dimensional vorticity equation with spectral truncation on a rectangular domain. For a sufficiently large number of degrees of freedom, the equilibrium statistics of the flow can be described through a canonical ensemble with two conserved quantities, energy and enstrophy. To perturb the system out of equilibrium, we change the shape of the domain according to a protocol, which changes the kinetic energy but leaves the enstrophy constant. We interpret this as doing work to the system. Evolving along a forward and its corresponding backward process, we find numerical evidence that the distributions of the work performed satisfy the Crooks relation. We confirm our results by proving the Crooks relation for this system rigorously.

DOI: 10.1103/PhysRevLett.110.234502 PACS numbers: 47.52.+j, 47.11.Kb, 05.70.Ln

The second law of thermodynamics states that the average work necessary to move a thermodynamic system, coupled to a heat bath, from one state of thermal equilibrium to another is bounded by the free energy difference between the final and initial state, $\langle W \rangle \geq \Delta F$. Here, equality holds for reversible processes only. The additional amount of work depends on the protocol. In many situations, though, a more detailed relation for the statistics of this work holds, known as Crooks relation [1]:

$$\frac{P_f(W)}{P_b(-W)} = e^{\beta(W-\Delta F)}. \quad (1)$$

Here, $P_f(W)$ denotes the probability density of the work obtained in the forward process, while $P_b(W)$ is the density of the work obtained in the backward process (i.e., under a time reversed protocol). The ratio is given in terms of the inverse temperature β and the free energy difference ΔF, i.e., parameters of the equilibrium of the system, only. Relation (1) may hold arbitrarily far from equilibrium. As of today, the Crooks relation, together with the Jarzynski relation [2], provides a very important generalization of thermodynamic work theorems into the fully nonequilibrium regime. Investigation into these relations and refinements is ongoing, see, e.g., [3,4]. The Crooks relation has been investigated in a number of situations, either numerically, analytically or experimentally [5–12].

We demonstrate that Eq. (1) holds for a two-dimensional inviscid and incompressible flow on a rectangular domain. The only physical parameter of this system, apart from those set by initial conditions, is the shape of the domain, which we change in order to drive the system out of equilibrium. This entails changes in the kinetic energy, which are interpreted as work. In our situation the fluctuations of the work are not due to random forces exerted by a heat bath, but are caused by chaoticity of the dynamics. By describing the flow in equilibrium through a canonical ensemble, we obtain the parameters β and ΔF for Eq. (1). One should keep in mind that the system is not thermodynamic in the classical sense; and whether β should be considered an inverse temperature is a matter of interpretation. We will nonetheless refer to it as Crooks relation. We demonstrate the Crooks relation numerically and prove it rigorously at the end of this Letter. The numerical results show interesting details which are not revealed by the proof and are therefore included.

An inviscid and incompressible flow on a two-dimensional Riemannian manifold $\mathcal{M}$ obeys the vorticity equation,

$$\partial_t \omega = \frac{1}{g}(-\partial_x \psi \partial_y \omega + \partial_y \psi \partial_x \omega), \qquad \Delta \psi = \omega. \quad (2)$$

Here, ψ is the stream function, which gives the velocity as $v^i = g^{-1}(-\partial_y \psi, \partial_x \psi)$, $i = 1,2$; and ω is the vorticity. This guarantees $\mathrm{div}(v) = g^{-1}\partial_i(g v^i) = 0$. Further, g is the Riemannian volume, and Δ is the Laplacian with respect to the Riemannian metric tensor g_{ij}.

The physical parameters of this equation are the entries of the metric tensor. We consider a situation in which the metric tensor is time dependent, but in a way that leaves the Riemannian volume g constant. (Otherwise, the notion of incompressibility would need to be reinterpreted.) Starting from the principle of least action, it can be shown that in this situation the vorticity equation still applies. (The Euler equations though will contain another term, reflecting the time dependence of the metric.)

In this Letter $\mathcal{M}$ is a simple rectangle of size $L \times 1/L$. Here, g equals one. For a point (x, y) on $\mathcal{M}$ we use coordinates $\xi = x/L$, $\eta = yL$, in order to make flows on different domain sizes easily comparable. The vorticity equation in this setting now reads:

$$\partial_t \omega = -(\partial_\xi \psi \partial_\eta \omega - \partial_\xi \psi \partial_\eta \omega), \quad (3)$$

$$\left(\frac{1}{L^2}\partial_\xi^2 + L^2 \partial_\eta^2\right)\psi = \omega. \quad (4)$$

Two important characteristics of the flow are its kinetic energy E and its enstrophy Γ^2, defined as

$$E = \frac{1}{2}\int dV g g_{ij} v^i v^j = \frac{1}{2}\int_0^1 \int_0^1 d\xi d\eta \psi \omega, \quad (5)$$

$$\Gamma^2 = \int dV g \omega^2 = \int_0^1 \int_0^1 d\xi d\eta \omega^2. \quad (6)$$

They are conserved by the dynamics as long as the metric, i.e., L, is kept constant.

Each time-dependent choice $L(t)$ will be volume-preserving by construction. Therefore the enstrophy will stay constant during time evolution but the energy will not. It changes according to

$$\frac{dE}{dt} = -\frac{\dot{L}}{L}\int d\xi d\eta \left(\frac{\partial_\xi^2 \psi}{L^2} - \partial_\eta^2 \psi L^2\right)\psi. \quad (7)$$

The evolution of the kinetic energy depends on the microstate of the flow, more specifically, on ψ and its second derivatives. Even for fields ω having initially the same energy, the energy change is different as it depends on the details of $\omega(\xi, \eta, t)$.

In our simulations we solve Eqs. (3) and (4) with time-dependent $L(t)$ numerically. We use a pseudospectral method with a truncated Fourier series of the vorticity with $N \times N$ complex Fourier amplitudes Ω_{kl}. The ordinary differential equation (ODE) for the Fourier amplitudes Ω_{kl} is integrated with a Runge Kutta scheme of fourth order with adaptive step size. The wave numbers included are all k, l with $0 < k^2 + l^2 < K^2$ and $K = 26$. For all the results shown here we use a doubly periodic domain. (Everything still applies for boundary conditions that prohibit flow through the boundaries.) In this approach, the integral formulations of energy, Eq. (5), and enstrophy, Eq. (6), are replaced by sum formulas. An important property of the truncated equations is that energy and enstrophy remain conserved quantities for constant L.

There exists a number of approaches trying to characterize the equilibrium of two-dimensional inviscid and incompressible fluid flow, which emphasize different features (see, e.g., [13,14]; or [15] and references therein for an overview). The one used in the present context is most suited to describe a truncated fluid flow. It characterizes the equilibrium of the flow by a generalized canonical ensemble of the dynamically conserved quantities energy and enstrophy, according to [16,17]. This ansatz provides a good approximation of the relevant momenta of the complex Fourier amplitudes for equal to or more than 16×16 grid points [18,19]. The density of states for the generalized canonical ensemble is written as the inverse partition function Z times an exponential term,

$$\mathbb{P}(\{\Omega_{kl}\}) = \frac{1}{Z}\exp[-\alpha\Gamma^2(\{\Omega_{kl}\}) - \beta E(\{\Omega_{kl}\})]. \quad (8)$$

Here, α and β are Lagrangian multipliers preserving the expectation values of energy and enstrophy. The density splits into a product of densities of states for the complex amplitude of each mode Ω_{kl}, and can be integrated. Both the real and imaginary part of a mode Ω_{kl} have a Gaussian distribution with zero mean and standard deviation $\sigma_{kl}(L, \alpha, \beta)$. The mean values of energy and enstrophy (and their spectra) are given through α and β. The density is normalizable even if either α or β is negative. Further details can be found in [16,17]. Even though there is no discontinuous change of property between the three regimes, where either α or β is negative or both are positive [17], we numerically checked our results in all three regimes. The region of most interest is, where $\beta < 0$, because there the energy per wave number decreases for an increasing wave number. Fields from this regime give the best approximation to real fluid fields (with low viscosity), where the excitation of the highest wave numbers can be neglected (see [17,20]). For $\beta < 0$ the equilibrium statistics introduced here can be connected to typical turbulence phenomena [21].

To characterize the nonequilibrium we explore the change of a field's kinetic energy during a process with time-dependent $L(t)$. We sample fields from the generalized canonical distribution, Eq. (8). For this we have to fix the Lagrangian multipliers α and β as well as L. One could think of canonically prepared fields, which are decoupled from the reservoirs α and β while running the process. Speaking about reservoirs should emphasize the analogy to a physical system (e.g., of particles), which are coupled to a heat bath of inverse temperature β, which motivates the choice of this ensemble.

The values we choose are $\alpha = 3$, $\beta = -60$, and a quadratic domain size, i.e., $L = 1$. We apply a protocol to each of these fields, where we linearly change the domain length (and inversely the height) $L(t) = 1 + ht$ for $t \in [0, t_e = \Delta/h]$. The parameter h is the speed of the process and Δ the maximal difference between the length of the rectangle and the square. Figure 1 shows a scatter plot of each field's final energy over its initial energy for two different protocol speeds h. Two characteristics should be pointed out: First, different fields with the same initial energy (i.e., which lie on one vertical line in Fig. 1) will end up with different final energies, because the change in energy depends on the details of the entire field (see equation (7), and text below). Second, the distribution for the slow process (blue dots) lies nearly fully within the

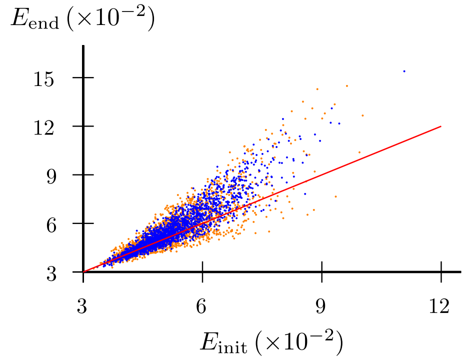

FIG. 1 (color online). Scatter plot of each field's final energy over its initial energy. (Sample size: 2000) Fields are sampled from a canonical distribution with $\alpha = 3$, $\beta = -60$. The simulated process is $L(t) = 1 + ht \in [1, 1.5]$ with two different speeds $h = 0.05$ (blue dots) and $h = 0.5$ (orange dots). The red line indicates equal initial and final energy.

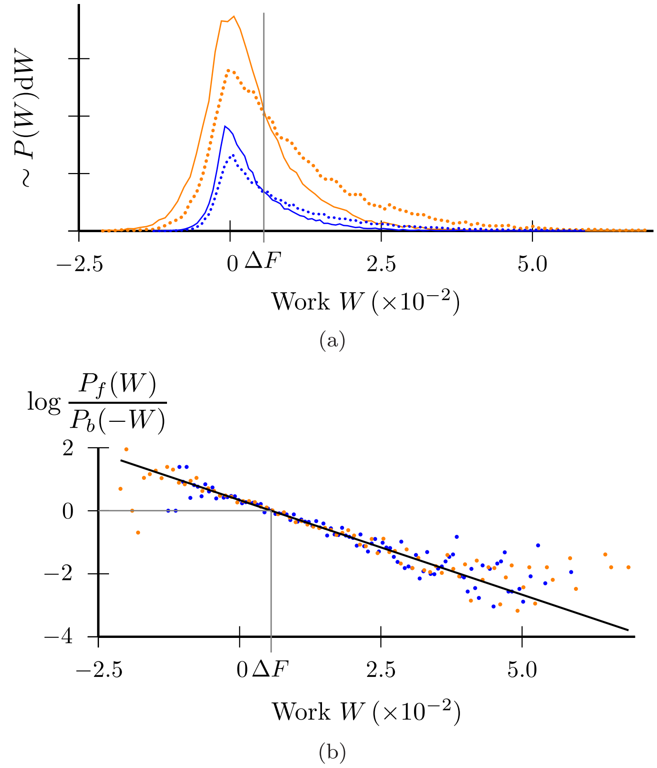

FIG. 2 (color online). The Crooks relation for a double periodic domain with fields chosen from a canonical distribution. Parameters: $\alpha = 3$, $\beta = -60$, $\Delta = 0.5$, $h = 0.05$ (blue), $h = 0.5$ (orange). $\Delta F = 5.60029 \times 10^{-3}$ [Eq. (9)]. (a) Work distributions from deforming the domain from square to rectangle. Solid line: Forward process; Dotted line: Backward process [distribution of negative work $P_b(-W)$]. The ordinate has different scales for the blue and the orange distributions to facilitate presentation. (b) Dots: Ratio of the numerically sampled work distributions, plotted on a logarithmic scale. Solid line: Right-hand side of Eq. (1) for parameters as given above.

distribution of the fast process (orange dots), because in a slower process the fluctuations in the energy have more time to cancel out each other.

To probe the Crooks relation, a backward process has to be performed. Vorticity fields stem from a generalized canonical distribution with the same α and β as in the forward process, but this time rectangular domain size $L = 1 + \Delta$. The inverse protocol is run, $L(t_e - t)$. Thereby, work distributions are obtained, where the work is defined as $W = E_{\rm end} - E_{\rm init}$. The distributions of the work in the forward and backward process should fulfill the Crooks relation, Eq. (1). For our system, we still need to define the free energy used in Eq. (1). We do this in formal analogy to the canonical ensemble as $-(1/\beta)\log Z$. The free energy difference ΔF is then calculated:

$$\Delta F = \frac{1}{\beta}\log\left(\frac{Z_1}{Z_{1+\Delta}}\right) \tag{9}$$

with Z being the partition function as introduced in Eq. (8). The indices 1 and $1 + \Delta$ indicate which values L have to be used to calculate Z. We name the quantity F free energy, knowing full well that this term usually defines a thermodynamic potential depending on temperature and volume. One could think of replacing the variable for the volume by the variable for the enstrophy. However, this definition of the free energy (difference) is justified. As we shall see later on, the value calculated through Eq. (9) is exactly the intersection point of the work distributions fulfilling the Crooks relation, i.e., the number which is represented by ΔF in Eq. (1) [see Fig. 2(a)].

One could extend Eq. (1) by a term $e^{-\alpha\Delta\Gamma^2}$ to generalize the equation to a system with a second reservoir, as it is the case here (see [1]). Because the enstrophy does not change during the process, this additional term is not necessary.

The work distributions are obtained from sampling 20 000 fields. In the process we apply the protocols introduced above with several different velocities h. Consider Fig. 2(a), where we present the results for the system with $\alpha = 3$, $\beta = -60$. Shown are the probability density functions (approximated by histograms) of the (positive) work distribution in the forward and the negative work distribution in the backward process. This is done for a slow process (in blue) and a faster one (in orange). The distributions are highly asymmetric and far from being Gaussian. For most experiments and simulations that have been reported in the literature, the maxima of the distributions are somewhat separated, with the graphs intersecting at a point in between (see [5–9]). Here, however, the maxima are very close to each other, with the point of intersection further away to the right of both. Notice that indeed this point of intersection is given by the free energy difference calculated through Eq. (9).

Calculating the expectation value of the work in the distributions shown in Fig. 2(a), one finds that it is actually *smaller* than ΔF (or resp. $\langle W\rangle \leq -\Delta F$ in the backward process), thus apparently violating the second law. The reason for this behavior is the negative temperature. In

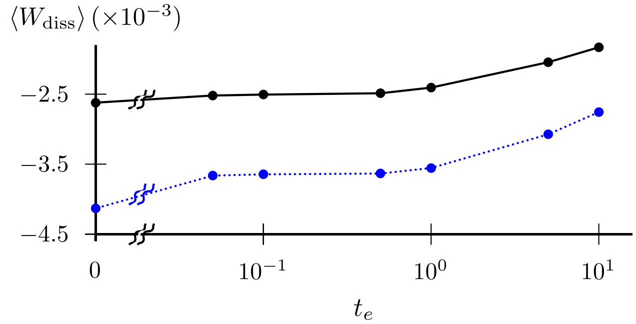

FIG. 3 (color online). This graph shows the average dissipated work in the forward (black) and backward (blue) process, versus the total time of the protocol t_e.

fact, using the Crooks relation and Jensen's inequality one gets $0 \leq \beta(\langle W\rangle - \Delta F)$ for any β. This gives $\langle W\rangle \geq \Delta F$ for positive temperature but $\langle W\rangle \leq \Delta F$ in our case. The difference is usually referred to as the dissipated work $W_{\mathrm{diss}} = W - \Delta F$. See Fig. 3. This figure also shows that the absolute value of the mean of the dissipated work decreases for slower processes. This supports the analogy to "ordinary" thermodynamic systems, where the absolute value of the mean of the dissipated work decreases when slowing down the protocol in order to reach the reversible limit ($\langle W_{\mathrm{diss}}\rangle = 0$) for an infinitely slow process.

Introducing the dissipated work we want to emphasize that we do not simulate a complete thermodynamic cycle, but only the parts where the protocols are applied. Because the system considered here is thermally isolated during the process, all work, which was not used to overcome the free energy difference, would be dissipated by bringing the system in contact with a heat bath after the protocol has finished. This thermalization is not simulated explicitly here (especially as it is not clear what this would mean in terms of evolution equations for the flow), but mimicked by simply discarding the fluid fields in favor of another independent sample from the canonical distribution in order to initialize a simulation in the reverse direction.

Considering the highly asymmetric distributions of Fig. 2(a), it seems even more surprising that the Crooks relation indeed holds for these distributions. In Fig. 2(b) we show the logarithm of the ratio of the bar heights of the histogram (points). The solid line is not a fit, but the linear function $\beta(W - \Delta F)$ with β being the Lagrangian multiplier determining the initial ensemble, and ΔF given by Eq. (9). It fits both the blue and the orange dots reasonably well. This is clear evidence that the Crooks relation holds for the kind of process considered. The larger deviations for low or high values of work are due to the low number of events with the corresponding work. One may get the impression that the deviations are systematically above the solid line on the right end and below the solid line on the left end. This is correct. The reason for this is that the values on the ordinate are logarithms of ratios of positive integers. If either the denominator or the numerator is zero, the ratio is not plotted. Doing this, one systematically overestimates the numerator (for high values of W) resp. the denominator (for low values of W) and is thus systematically above resp. below the solid line.

In our situation, the Crooks relation can even be demonstrated rigorously. We will provide a sketch of the proof, only. The truncated vorticity equation essentially amounts to a system of ordinary differential equations $\dot{x} = v(t, x)$. The time dependence of the latter is due to parameters of the equation being changed according to a protocol $\lambda(t)$. If we specify an initial time t_s and some initial point $x \in \Sigma$, then integrating this ODE to some terminal time t_e gives a terminal point $\Phi(x) \in \Sigma$. The mapping Φ so defined (to which we refer as the *forward flow*) is a diffeomorphism on Σ. Furthermore, since $\mathrm{div}(v) = 0$, the Jacobian of Φ is one. Integrating the ODE backward under the time reversed protocol, we obtain the *backward flow* $\Psi(x) = \iota \circ (\Phi)^{-1} \circ \iota(x)$, where simply $\iota(x) = -x$. Necessarily, the Jacobian of $\Psi(x)$ is one, too. Let E_λ be the energy, which is invariant under ι. The *work* of the forward resp. backward flow are defined as $W_f(x) = E_1 \circ \Phi(x) - E_0(x)$, $W_b(x) = E_0 \circ \Psi(x) - E_1(x)$, respectively. Due to the invariance of the energy with respect to ι, we have that $W_b \circ \iota \circ \Phi(x) = -W_f(x)$. Further, let Γ^2 be the enstrophy, which does not depend on the parameter and is invariant under both ι and the flow. Using the energy and the enstrophy, we now introduce the (generalized canonical) probability distributions

$$d\mathbb{P}_\lambda = e^{S_\lambda(x)}dx, \qquad S_\lambda(x) = \beta[F_\lambda - E_\lambda(x)] - \alpha\Gamma^2(x).$$

With these prerequisites, it can be shown that for any function ϕ,

$$\mathbb{E}_0[\phi(W_f)] = \mathbb{E}_1[\phi(-W_b)e^{-\beta(W_b+\Delta F)}], \tag{10}$$

where $\mathbb{E}_0$, $\mathbb{E}_1$ are the expectation values with respect to $\mathbb{P}_0$, $\mathbb{P}_1$, respectively. Equation (10) implies the Crooks relation. The proof of Eq. (10) is as follows:

$$\begin{aligned}
&\mathbb{E}_0[\phi(W_f)]\\
&\quad= \int_\Sigma \phi(W_f(x))e^{S_0(x)}dx\\
&\quad= \int_\Sigma \phi(W_f(x))e^{S_0(x)-S_1\circ\Phi(x)}e^{S_1\circ\Phi(x)}dx\\
&\quad= \int_\Sigma \phi(W_f(x))e^{\beta W_f(x)-\beta\Delta F}e^{S_1\circ\Phi(x)}dx\\
&\quad= \int_\Sigma \phi(-W_b\circ\iota\circ\Phi(x))e^{-\beta(W_b\circ\iota\circ\Phi(x)+\Delta F)}e^{S_1\circ\Phi(x)}dx\\
&\quad= \int_\Sigma \phi(-W_b(x))e^{-\beta(W_b(x)+\Delta F)}e^{S_1(x)}dx\\
&\quad= \mathbb{E}_1[\phi(-W_b)e^{-\beta(W_b+\Delta F)}].
\end{aligned}$$

To summarize, we have successfully verified the Crooks fluctuation theorem, Eq. (1), for an inviscid two-dimensional flow, both numerically as well as analytically. This is remarkable, for two reasons, first since the fluctuations in the system are not the consequence of a stochastic process, but the outcome of deterministic equations which generate turbulent and mixing behavior of the fluid field. Second, the Crooks relation holds despite highly asymmetric distributions of the work performed on the system. This numerical experiment was run with considerably low numerical resolution in order to provide a sufficiently large sample. However, the outcome can be considered as a point of reference for computationally expensive simulations or for real fluid experiments, especially with low viscosity.

*Corresponding author.
juguma@pks.mpg.de

[1] G. E. Crooks, Phys. Rev. E **60**, 2721 (1999).
[2] C. Jarzynski, Phys. Rev. Lett. **78**, 2690 (1997).
[3] R. Kawai, J. M. R. Parrondo, and C. Van den Broeck, Phys. Rev. Lett. **98**, 080602 (2007).
[4] M. Esposito and C. Van den Broeck, Phys. Rev. Lett. **104**, 090601 (2010).
[5] F. Douarche, S. Ciliberto, and A. Petrosyan, J. Stat. Mech. (2005) P09011.
[6] D. Collin, F. Ritort, C. Jarzynski, S. B. Smith, I. Tinoco, Jr., and C. Bustamante, Nature (London) **437**, 231 (2005).
[7] P. Procacci, S. Marsili, A. Barducci, G. F. Signorini, and R. Chelli, J. Chem. Phys. **125**, 164101 (2006).
[8] H. Híjar, J. Quintana-H, and G. Sutmann, J. Stat. Mech. (2007) P04010.
[9] L. Granger, M. Niemann, and H. Kantz, J. Stat. Mech. (2010) P06029.
[10] K. Hayashi, H. Ueno, R. Iino, and H. Noji, Phys. Rev. Lett. **104**, 218103 (2010).
[11] G. Gradenigo, A. Puglisi, A. Sarracino, and U. M. B. Marconi, Phys. Rev. E **85**, 031112 (2012).
[12] O.-P. Saira, Y. Yoon, T. Tanttu, M. Möttönen, D. V. Averin, and J. P. Pekola, Phys. Rev. Lett. **109**, 180601 (2012).
[13] R. Robert and J. Sommeria, J. Fluid Mech. **229**, 291 (1991).
[14] L. Onsager, Nuovo Cimento **6**, 279 (1949).
[15] F. Bouchet and A. Venaille, Phys. Rep. **515**, 227 (2012).
[16] R. H. Kraichnan, J. Fluid Mech. **67**, 155 (1975).
[17] D. G. Fox and S. A. Orszag, Phys. Fluids **16**, 169 (1973).
[18] C. Basdevant and R. Sadourny, J. Fluid Mech. **69**, 673 (1975).
[19] L. C. Kells and S. A. Orszag, Phys. Fluids **21**, 162 (1978).
[20] R. H. Kraichnan, Phys. Fluids **10**, 1417 (1967).
[21] E. A. Novikov, Arch. Mech. Warsaw **26**, 741 (1974).